

# Enhanced Lipid and Biodiesel Production from Glucose-Fed Activated Sludge: Kinetics and Microbial Community Analysis

Andro H. Mondala, Rafael Hernandez, Todd French, and Linda McFarland

Renewable Fuels and Chemicals Laboratory, Dave C. Swalm School of Chemical Engineering, Mississippi State University, MS 39762

Jorge W. Santo Domingo, Mark Meckes, Hodon Ryu, and Brandon Iker

U.S. Environmental Protection Agency, Office of Research and Development, National Risk Management Research Laboratory, Cincinnati, OH 45268

DOI 10.1002/aic.12655

Published online May 6, 2011 in Wiley Online Library (wileyonlinelibrary.com).

*An innovative approach to increase biofuel feedstock lipid yields from municipal sewage sludge via manipulation of carbon-to-nitrogen (C:N) ratio and glucose loading in activated sludge bioreactors was investigated. Sludge lipid and fatty acid methyl ester (biodiesel) yields (% cell dry weight, CDW) were enhanced via cultivation in activated sludge bioreactors operated at high initial C:N ratio ( $\geq 40:1$ ) and glucose loading ( $\geq 40 \text{ g L}^{-1}$ ). Under C:N 70, 60  $\text{g L}^{-1}$  glucose loading, a maximum of  $17.5 \pm 3.9$  and  $10.2 \pm 2.0\%$  CDW lipid and biodiesel yields, respectively, were achieved after 7 d of cultivation. The cultured sludge lipids contained mostly  $C_{16}$ – $C_{18}$  fatty acids, with oleic acid consistently accounting for 40–50% of the total fatty acids. Microbial composition in activated sludge exposed to C:N 70 shifted toward specific gammaproteobacteria, suggesting their relevance in lipid production in wastewater microbiota and potential value in biofuel synthesis applications. © 2011 American Institute of Chemical Engineers AIChE J, 58: 1279–1290, 2012*

**Keywords:** energy, environmental engineering, fermentation, mathematical modeling, green engineering

## Introduction

Government initiatives and scientific research geared toward the development of biomass-based alternative fuels such as biodiesel and green diesel have been increasing in recent years due to the impact of greenhouse gas emissions from the combustion of fossil fuels, increasing petroleum prices, and energy security concerns associated with the United States' continued reliance on foreign oil.<sup>1</sup> Biodiesel

is produced by the transesterification of vegetable oils and animal fats with an alcohol such as methanol to yield the corresponding esters of the fatty acids comprising the lipid feedstock.<sup>2</sup> On the other hand, Green diesel is considered a second generation biofuel produced from the catalytic hydrogenation of lipids containing triglycerides and/or free fatty acids.<sup>3,4</sup> However, the use of crop oils such as soybean oil as feedstock presents several challenges such as variations in lipid quality and potential supply interruptions due to location, season, disease, pests, weather conditions, and climate change.<sup>5</sup> There are also concerns about food security and rising food costs due to utilization of these feedstocks for non-food uses, impact on landscape ecology, and land demands

Correspondence concerning this article should be addressed to R. Hernandez at rhernandez@che.msstate.edu or T. French at french@che.msstate.edu.

associated with the production of specific crops.<sup>6</sup> In the case of biodiesel, production costs are currently higher than petroleum diesel due to high cost of refined vegetable oil feedstocks, which typically constitutes 70–85% of the overall biodiesel production cost.<sup>7</sup> Due to these limitations, it is important to explore low-cost, nonfood-based lipid feedstocks that are available all year round as potential biofuel raw materials.

Recently, municipal sewage sludge has been gaining considerable attention as a potential biodiesel feedstock.<sup>8–11</sup> Sewage sludges contain a significant lipid fraction composed of absorbed fats and oils as well as microbial phospholipids. Moreover, the US Environmental Protection Agency (EPA) estimated that 7.6–8.2 M dry tons of sludge are produced in the United States annually.<sup>12</sup> Despite this abundant supply, investigating the potential of biodiesel production from sewage sludge-derived lipids has been limited to a few studies. Dufreche et al.<sup>9</sup> obtained a 27.4% (w/w dry sludge) lipid yield following lipid extraction of primary and activated sludge from a municipal wastewater treatment plant (WWTP). Subsequent transesterification of the lipid extracts yielded 4.41% biodiesel (w/w dry sludge). Using sewage sludge obtained from the same WWTP, Mondala et al.<sup>10</sup> achieved maximum biodiesel yields of 14.5 and 2.5% (w/w dry sludge) via in situ transesterification of primary and activated sludges, respectively. Additionally, Revellame et al.<sup>11</sup> obtained a maximum biodiesel yield of 4.79% (w/w dry sludge) from activated sludge at optimum in situ transesterification conditions. Based on these results, it is of interest to increase the lipid content of sewage sludge to make it more competitive with conventional oil crops as biodiesel feedstocks in terms of biodiesel yield.

In this paper, an innovative strategy to enhance lipid production in activated sludge microorganisms based on the concept of lipid accumulation in oleaginous microorganisms is presented. The latter are known to accumulate 20–70% lipids (cell dry weight, CDW) in response to high carbon and nitrogen-limited conditions (i.e., high C:N).<sup>13,14</sup> As the sewage sludge utilized in previous transesterification studies were obtained from an activated sludge reactor operating at low carbon ( $\text{COD} = 394 \pm 94 \text{ mg L}^{-1}$ ) and low nitrogen ( $\text{NH}_4^+ - \text{N} = 22 \pm 3 \text{ mg L}^{-1}$ ,  $\text{NO}_2^- - \text{N} = 4.2 \pm 0.9 \text{ mg L}^{-1}$ ) conditions, it was hypothesized that certain members of the activated sludge microbiota would accumulate additional lipids under high C:N and substrate loading, thereby increasing the amount that could be extracted from sludge and converted to biodiesel.

The main objectives of this study were to determine the effects of initial C:N ratio (10:1 to 70:1) and glucose loading ( $20\text{--}60 \text{ g L}^{-1}$ ) on biomass production, lipid accumulation, and glucose consumption by wastewater microbiota grown in aerobic activated sludge bioreactors. Lipid extracts from sludge biomass were transesterified to determine biodiesel yield and fatty acid profiles. Mathematical models that describe the process were proposed and fitted to the experimental data to obtain kinetic parameters needed for process scale-up and bioreactor design and to develop quantitative descriptions of microbial growth, product formation, and substrate utilization occurring during the fermentation process. Variations in the microbial composition were investigated using sequence analysis of 16S rRNA gene clone

**Table 1. Experimental Design Used in This Study**

Treatment No.	C:N Ratio	Glucose Loading ( $\text{g L}^{-1}$ )	Ammonium Sulfate ( $\text{g L}^{-1}$ )
1	10:1	60	11.3
2	40:1	60	2.8
3	70:1	60	1.6
4	70:1	40	1.1
5	70:1	20	0.5

libraries to better understand the importance of microbial community structure of activated sludge in the lipid production process.

## Materials and Methods

### Activated sludge bioreactor setup

Activated sludge samples obtained from the municipal WWTP in Tuscaloosa, AL were used as inocula. Samples were collected in 500-mL plastic bottles and transported in ice coolers. Upon arrival at the laboratory, equal volumes of the grab sludge samples were mixed together to form a composite sample and maintained in a 3-L glass jar with mixing and aeration at room temperature.

A modified synthetic wastewater adapted from Ghosh and LaPara<sup>15</sup> was used as cultivation media for activated sludge. It contained the following components ( $\text{L}^{-1}$  of deionized water): gelatin 0.15 g, starch 0.21 g, yeast extract 0.07 g, casamino acids 0.01 g,  $\text{NaH}_2\text{PO}_4$  1.5 g,  $\text{K}_2\text{HPO}_4$  1.0 g, and trace mineral solution 5 mL. Glucose and ammonium sulfate were added as carbon and nitrogen sources, respectively, in amounts corresponding to different initial mass C:N ratios and substrate loadings (Table 1). The medium was sterilized by autoclaving at  $121^\circ\text{C}$ , 240 kPa for 20 min. Glucose was autoclaved separately to prevent caramelization and mixed aseptically with the rest of the media using aseptic techniques after cooling to room temperature. The initial pH of the media was then set to 6.5 using sterile  $5 \text{ mol L}^{-1}$  NaOH.

Batch cultivation experiments were conducted using a set of five 5-L BIOFLO 310/3000 Bioreactors (New Brunswick Scientific, Edison, NJ) with an initial working volume of 3 L. The pH of the culture was uncontrolled and monitored throughout the duration of the experiment using a built-in pH probe. The temperature of the culture was controlled at  $25 \pm 1^\circ\text{C}$  using a platinum resistance temperature detector (RTD) and a water jacket in the fermenter vessel. Foaming was prevented by the automatic addition of a 1:10 dilution of nonoil, polypropylene-based Antifoam 204 concentrate (Sigma–Aldrich, St. Louis, MO). Aerobic batch fermentation was commenced by inoculating the sterile media with 20% (v/v) of the maintained activated sludge. Air filtered through a  $0.45\text{-}\mu\text{m}$  HEPA vent filter (Whatman, Kent, UK) was bubbled into the culture at 1 vvm (volume of air per volume of media per minute). Agitation rate was set at 300 rpm in the first 24 h of fermentation and then increased to 400 rpm at 24 h and 500 rpm at 48 h to maintain a minimum dissolved oxygen level of 20% saturation throughout the experiment. The total incubation time for the batch culture was 7 d. Experimental treatments were tested simultaneously, and replicate experiments were conducted within 2–4 weeks.

## Analytical methods

Culture samples were collected at regular time intervals via an air-lock sampling port. Cell biomass concentration was measured by centrifuging 30-mL samples at 3400g for 20 min. The cell pellets were washed with 20 mL of 0.85% (v/v) saline solution and stored in a  $-80^{\circ}\text{C}$  freezer for at least 2 h. The frozen cell pellets were then freeze dried using a Freezone 6 Bulk Tray Freeze Dryer (Labconco, Kansas City, MO) and weighed. The results were reported as cell dry mass concentration.

Residual glucose in the supernatant was measured using a YSI 2700 Biochemistry Analyzer (YSI Life Sciences, Yellow Springs, OH) equipped with a glucose oxidase membrane probe. Residual ammonium-nitrogen ( $\text{NH}_4^+-\text{N}$ ) was determined using an ICS 3000 ion chromatograph (Dionex, Sunnyvale, CA) equipped with an IonPac CS16 cation exchange analytical column (250 mm  $\times$  4 mm) and CG16 guard column (50 mm  $\times$  4 mm) and a conductivity detector using a method described elsewhere.<sup>16</sup>

Biomass-associated lipids were extracted and weighed using the method of Bligh and Dyer.<sup>17</sup> The weights were then recorded and reported as the gravimetric lipid yield (% CDW). Biodiesel yield and fatty acid profile of the lipid extracts were estimated by transesterification of the lipid extracts followed by gas chromatography (GC) analysis of the resulting fatty acid methyl ester (FAME) derivatives.<sup>18</sup> Two milliliters of a 2% (v/v) sulfuric acid in methanol was added to the lipid samples, vortex-mixed, and incubated at  $60^{\circ}\text{C}$  in a water bath for 2 h. The samples were then cooled to room temperature and quenched with 5 mL of an aqueous solution containing 3% (w/v)  $\text{NaCHO}_3$  and 5% (w/v)  $\text{NaCl}$ . The methyl esters were extracted from the reaction mixture with two washings of 2 mL toluene containing 200 ng  $\mu\text{L}^{-1}$  of 1,3-dichlorobenzene as the internal standard and 100 ng  $\mu\text{L}^{-1}$  of butylated hydroxytoluene as an antioxidant. The toluene extracts were then dried by passing them through anhydrous sodium sulfate in a glass fiber filter and diluted as needed. Two microliters of the dried toluene extracts were injected at  $260^{\circ}\text{C}$  in splitless mode into an Agilent 6890 Gas Chromatograph (Agilent Technologies, Santa Clara, CA) equipped with a 30 m  $\times$  0.25 mm ID Restek 11023 Stabilwax DA capillary column (Restek, Bellefonte, PA) having a 0.25- $\mu\text{m}$  film thickness. The oven temperature was initially set at  $50^{\circ}\text{C}$  for 2 min, after which it was ramped at  $10^{\circ}\text{C min}^{-1}$  to  $250^{\circ}\text{C}$ , where it was held constant for 13 min. The FAMES were detected using a flame ionization detector (FID) operating at  $260^{\circ}\text{C}$  and using helium as carrier gas (14 psi, 53.5 mL  $\text{min}^{-1}$  flow rate). The instrument was calibrated using a standard FAME mixture containing  $\text{C}_8$ – $\text{C}_{24}$  methyl esters (Sigma-Aldrich, St. Louis, MO). The total FAME concentration was used to estimate the total biodiesel yield and saponifiable fraction based on the cell dry weight.

## Kinetic modeling

A mathematical model describing the kinetics of nonlipid biomass synthesis, lipid accumulation, and sugar utilization of activated sludge microorganisms in an aerobic batch fermentation process was used following an approach first employed to model the formation of extracellular microbial polysaccharides<sup>19,20</sup> and subsequently for the lipid accumulation of the

oleaginous yeast *Rhodotorula gracilis* CFR-1.<sup>21,22</sup> To distinguish cell growth of the activated sludge microbiota as opposed to storage lipid synthesis, the model was fitted into the nonlipid biomass concentration data, which is the difference between the total biomass and mass of lipid extracts. The nonlipid biomass synthesis rate was characterized using the Logistic equation (Eq. 1), which was derived from the Monod equation, and characterized growth in terms of the carrying capacity of the culture medium<sup>23</sup>:

$$\frac{dX}{dt} = \mu_{\max} X(t) \left( 1 - \frac{X(t)}{X_{\max}} \right) \quad (1)$$

where  $X$  ( $\text{g L}^{-1}$ ) is the nonlipid biomass concentration in the fermentation broth at any time  $t$  (h),  $\mu_{\max}$  ( $\text{h}^{-1}$ ) is the maximum specific growth rate,  $X_{\max}$  ( $\text{g L}^{-1}$ ) is the maximum nonlipid biomass concentration attainable corresponding to the maximum carrying capacity, and  $[1 - (X/X_{\max})]$  represents the unused carrying capacity.<sup>23</sup>

Lipid accumulation was characterized by a Luedeking–Piret equation (Eq. 2), which expresses the rate of lipid production as a function of the instantaneous nonlipid biomass concentration  $X$  and the growth rate (based on the nonlipid biomass):

$$\frac{dP}{dt} = nX + m \frac{dX}{dt} \quad (2)$$

where  $P$  ( $\text{g L}^{-1}$ ) is the lipid concentration in the fermentation broth at any time  $t$  (h), and  $m$  and  $n$  are empirical constants that may be used to describe growth- ( $m dX/dt$ ) and nongrowth-associated ( $nX$ ) product formation, respectively. Based on this, generalizations can be made whether lipid accumulation in activated sludge microbiota is growth-associated or nongrowth associated based on the relative magnitudes of  $m$  and  $n$ .

Glucose utilization by the activated sludge microbiota was also modeled by a Luedeking–Piret equation (Eq. 3), where the rate of glucose utilization is expressed as a function of the instantaneous nonlipid biomass growth, lipid formation rate, and a cell maintenance coefficient term:

$$-\frac{dS}{dt} = \frac{1}{Y_{X/S}} \frac{dX}{dt} + \frac{1}{Y_{P/S}} \frac{dP}{dt} + k_e X \quad (3)$$

where  $S$  ( $\text{g L}^{-1}$ ) is the residual glucose concentration in the fermentation broth at any time  $t$  (h),  $Y_{X/S}$ , and  $Y_{P/S}$  ( $\text{g g}^{-1}$  glucose consumed) refer to the nonlipid biomass and lipid yield coefficients, respectively, and  $k_e$  is the maintenance coefficient. Alternately, Eq. 3 can be written as:

$$-\frac{dS}{dt} = \alpha \frac{dX}{dt} + \beta X \quad (4)$$

where

$$\alpha = \left( \frac{1}{Y_{X/S}} + \frac{m}{Y_{P/S}} \right) \quad (5)$$

and

$$\beta = \left( \frac{n}{Y_{P/S}} + k_e \right) \quad (6)$$

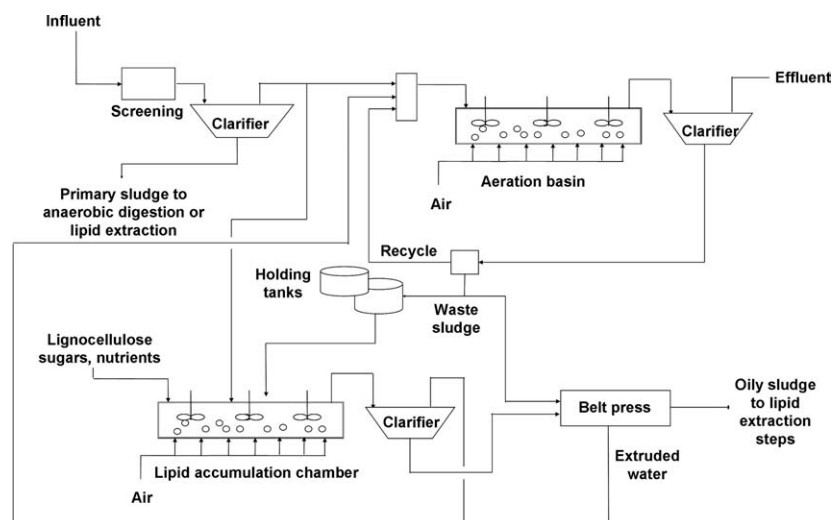


Figure 1. Proposed WWTP concept for the enhancement of lipid and biodiesel yields from activated sludge.

Values of the kinetic parameters found in the nonlinear expressions of  $X(t)$ ,  $P(t)$ , and  $S(t)$  obtained through integration of Eqs. 1–3 were estimated by iterative nonlinear least-squares regression using the Levenberg–Marquardt algorithm (Polymath® Professional 6.1, CACHE). The initial values used for the nonlinear regression were obtained from the linearized kinetics expressions using the calculation methods described in other papers.<sup>19–22</sup> Optimum values of the parameters were evaluated by the minimizing the sum of squares of the errors (i.e., the difference between the actual value of the dependent variable and the calculated value of the dependent variable from the model expression).

Validation of the proposed kinetics model was carried out by comparing the batch experimental data with simulated profiles of nonlipid biomass, lipid, and glucose concentration. The model simulations were obtained using the Runge–Kutta–Fehlberg (RK45) algorithm of the ordinary differential equations program of Polymath Professional 6.1 (CACHE). The performance of the proposed model was evaluated by calculation of the coefficient of determination:

$$R^2 = 1 - \frac{\sum (y_i - y_p)^2}{\sum (y_i - \bar{y}_i)^2} \quad (7)$$

where  $y_i$  and  $y_p$  are the experimental and model data, respectively.

### Microbial community analysis

Analysis of activated sludge microbial communities was performed using sequence analysis of 16S rRNA gene clone libraries.<sup>24,25</sup> Activated sludge culture samples (2 mL) were collected at different time intervals and concentrated by centrifugation (13,400g, 5 min). The supernatant was then discarded, and the cell pellets were stored at  $-80^\circ\text{C}$  until further processing. DNA was extracted using PowerSoil® DNA isolation kits (Mo Bio Laboratories, Carlsbad, CA) following manufacturer's instructions. DNA extracts were used in polymerase chain reaction (PCR) assays using universal primers 8F and 787R. PCR products were cloned and sequences ana-

lyzed as described elsewhere.<sup>25</sup> Clone libraries were developed for sludge samples prior to the treatments ( $t = 0$ ) and for each of the treatments at days 3 and 7 of cultivation. Sequences were classified and relative abundance of microbial groups were determined using LIBCompare software.<sup>26</sup>

### Results and Discussion

The WWTP configuration (Figure 1) suggested in this study utilizes the microbial community in municipal sewage activated sludge in an aerobic fermentation process to enhance the accumulation of storage lipids that could be used for the production of biodiesel. To our knowledge, this strategy has not previously been attempted, and therefore the kinetic data for biomass production, lipid accumulation, glucose utilization, and temporal changes in microbial composition are for the first time described. Fermentation profiles at different initial C:N ratios and initial glucose loadings are shown in Figures 2 and 3, respectively. The error bars in the figures represent the 90% confidence limits of the mean responses of four replicate experimental runs of the treatments investigated. Comparison of the model predictions and experimental data are illustrated and shown in Figure 4, and Figure 5 shows the relative proportions of total and saponifiable lipids in the raw and enhanced sludge extracts. The calculated kinetic parameters with their corresponding 90% confidence limits for all treatments investigated are summarized in Table 2.

### Effect of C:N ratio

High C:N ratio has been shown to stimulate the increase of lipid production in different microorganisms.<sup>27</sup> However, most studies involving oleaginous yeasts report C:N ratios between 30:1 and 80:1, most commonly around 40:1.<sup>28</sup> In this study, the resulting fermentation profiles indicate that increasing C:N ratio has a negative effect on the total biomass yield (Figure 2a). As the initial glucose supply was constant at  $60 \text{ g L}^{-1}$ , the increased biomass yield at C:N 10:1 and 40:1 compared to C:N 70:1 was affected primarily



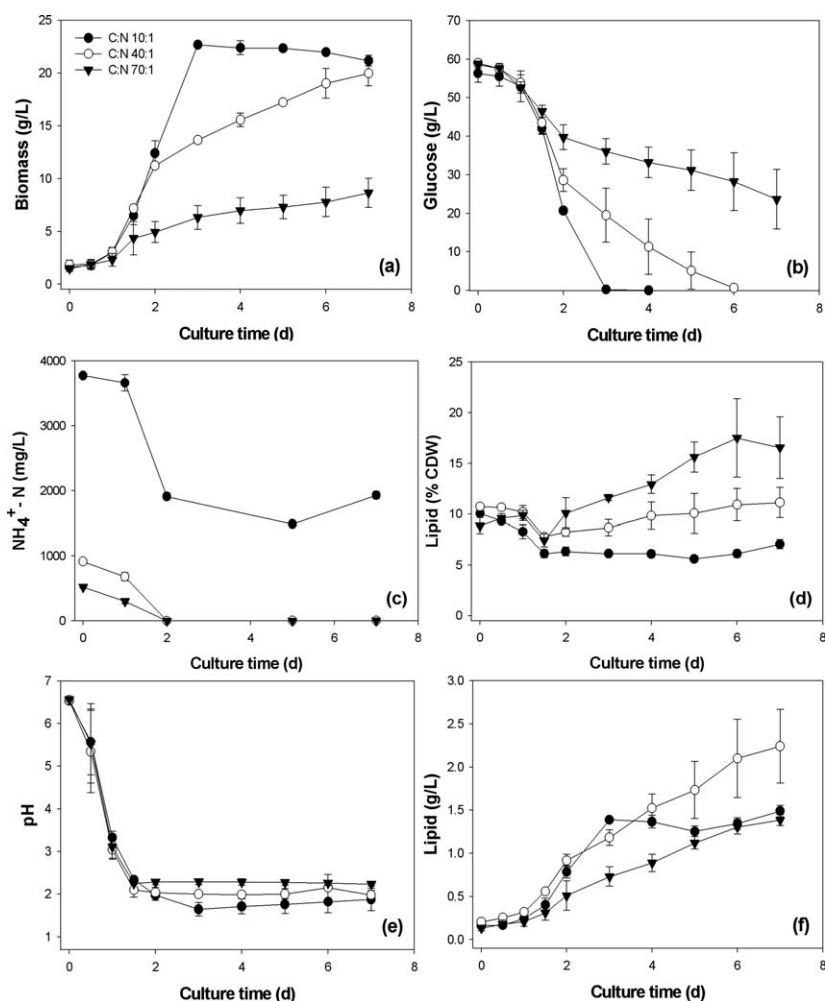


**Figure 2.** Fermentation profiles of activated sludge cultivated at  $60 \text{ g L}^{-1}$  initial glucose loading and different initial C:N ratios.

by the higher initial amounts of  $\text{NH}_4^+\text{—N}$  in the culture medium. A lag phase was observed during the first 24 h of fermentation in all C:N ratios investigated, after which the duration of the exponential phases and the observed cell growth rates differed significantly. At the C:N 10:1 culture, the exponential growth phase occurred at 2–3 d with a significantly faster growth rate than C:N 40:1 and 70:1 to reach the maximum biomass concentration. The biomass concentration then declined gradually due to the depletion of glucose at 3 d (Figure 2b) despite having  $\sim 2 \text{ g L}^{-1}$  residual  $\text{NH}_4^+\text{—N}$  in the fermentation broth (Figure 2c). At higher C:N ratios (40:1 and 70:1), the duration of the exponential phases was shorter (1–2 d) and was still followed by a gradual increase in the total biomass. In these C:N ratios, residual  $\text{NH}_4^+\text{—N}$  levels in the culture were found to be negligible at 2 d (Figure 2c), hence the observed increase in total biomass could be attributed to the increase in the lipid fraction.

Gravimetric lipid yield (in % CDW) profiles shown in Figure 2d indicate an initial reduction in the lipid content of the activated sludge coinciding with the lag phase. This probably occurred due to the mobilization of the initial lipid

reserves as readily available carbon source for the synthesis of enzymes for subsequent utilization of glucose by activated sludge microorganisms. After this initial lag phase at C:N 40:1, no significant increase in the lipid content was observed as shown by the error bars representing the 90% confidence limits of the mean. At C:N 10:1, the lipid content of the sludge biomass never recovered and stayed constant at  $\sim 7\%$  CDW. On the other hand, a significant increase in the lipid content was observed from the onset of the exponential phase (1.5–2 d) up to the early stationary phase (5 d) at the C:N 70:1 treatment run. This coincided with the depletion in  $\text{NH}_4^+\text{—N}$  levels in the culture as shown in Figure 2c; hence indicating oleaginity within some members of the activated sludge microflora. From 5 to 7 d of fermentation, the observed lipid contents were not significantly different and the maximum lipid content observed was  $17.5 \pm 3.9\%$  CDW. This is a marked improvement compared with raw activated sludge (RAS), which had average lipid content of  $11.0 \pm 1.7\%$  over the period of conducting this study. As the pH in the culture was not controlled, sharp declines in the culture pH from 6.5 to around 2.5 were observed in all experiments conducted (Figure 2e). This phenomenon could

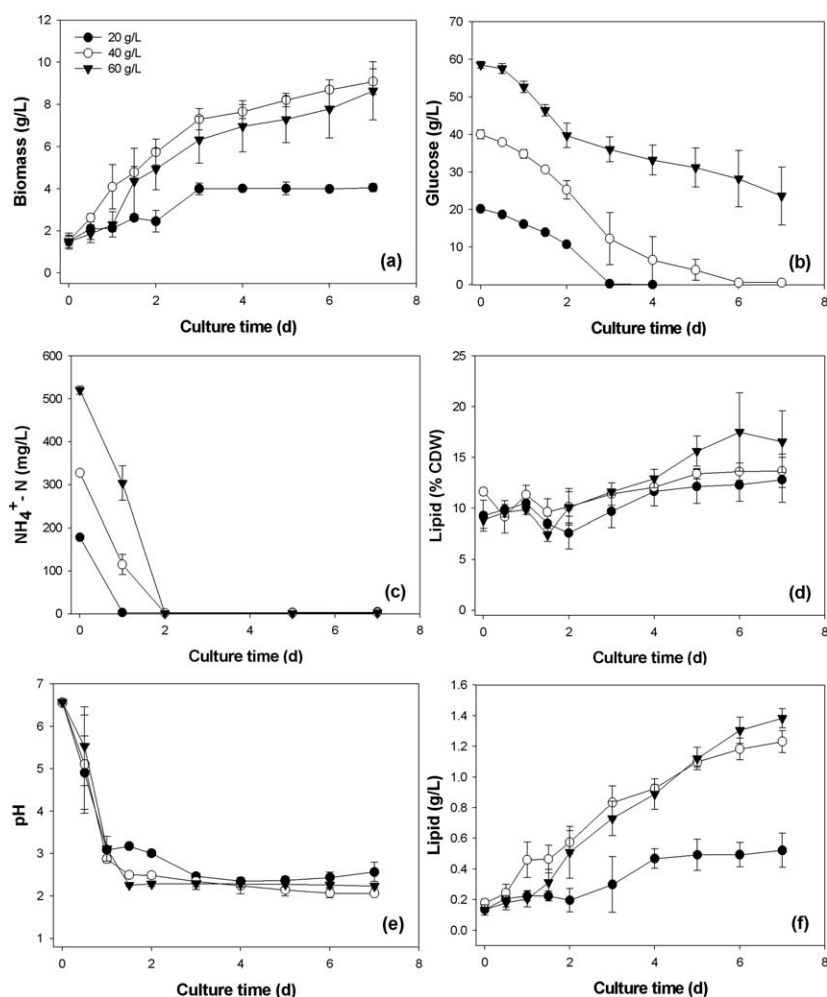


**Figure 3.** Fermentation profiles of activated sludge cultivated at C:N ratio 70:1 and different initial glucose loadings.

have been caused by one or more of the following: endogenous production of organic acids by the activated sludge microorganisms;<sup>23</sup> the release of acid in the culture with use of ammonium sulfate as the nitrogen source due to the preferential assimilation of  $\text{NH}_4^+$  radical;<sup>29</sup> and the formation of carbonic acid due to the dissolution of the  $\text{CO}_2$  produced by microorganisms into the culture.<sup>30</sup> Although it was previously reported that culture pH values below 3 reduced biomass and lipid production in pure cultures of oleaginous yeasts<sup>31</sup> and bacteria,<sup>32</sup> the results of this study showed that lipid accumulation in activated sludge occurred even at these very low pH levels, suggesting that some members of wastewater microbial communities are capable of accumulating lipids at these extreme conditions.

Despite having no significant enhancement in its gravimetric lipid content, activated sludge grown at C:N 40:1 showed higher volumetric lipid yields (in  $\text{g L}^{-1}$ ) as an effect of the increased total biomass production (Figure 2f). The same was observed initially at C:N 10:1 up to 3 d but started its decline along with the onset of the stationary phase. On the other hand, volumetric lipid yields in C:N 70:1-grown activated sludge exhibited an increasing trend, albeit at lower levels than C:N 40:1 despite having higher gravimetric lipid contents due to the lower biomass production. Furthermore,

the observed glucose consumption profiles (Figure 2b) indicated increasing rates of glucose uptake with decreasing C:N ratio due to the higher concentration of microbial cell biomass consuming the available glucose as substrate for growth and maintenance. Glucose was fully consumed after 3 d at C:N 10:1 and 6 d at C:N 40:1, whereas approximately one-third remained at C:N 70:1 after 7 d. This could indicate some substrate inhibition due to the high glucose residual relative to microbial cell concentration.

As shown in Table 2, the calculated  $\mu_{\text{max}}$  was highest at C:N 10:1 with no significant difference between C:N 40:1 and 70:1, while  $X_{\text{max}}$  and  $Y_{\text{X/S}}$  based on the nonlipid biomass also decreased with increasing C:N ratio at a constant initial glucose concentration of  $60 \text{ g L}^{-1}$ . The reduction in the biomass yield could then be attributed to the reduction of initial nitrogen supply needed for synthesis of cellular materials at higher C:N ratios. On the other hand, the maximum predicted volumetric lipid yield ( $P_{\text{max}}$ ) was highest at C:N 40, with no significant difference between C:N 10:1 and C:N 70:1. This was the case, although the overall lipid yield coefficient ( $Y_{\text{P/S}}$ ) estimates were not significantly different among the three C:N ratios investigated. These data suggest that the overall volumetric lipid yields of activated sludge microorganisms were more largely affected by cell

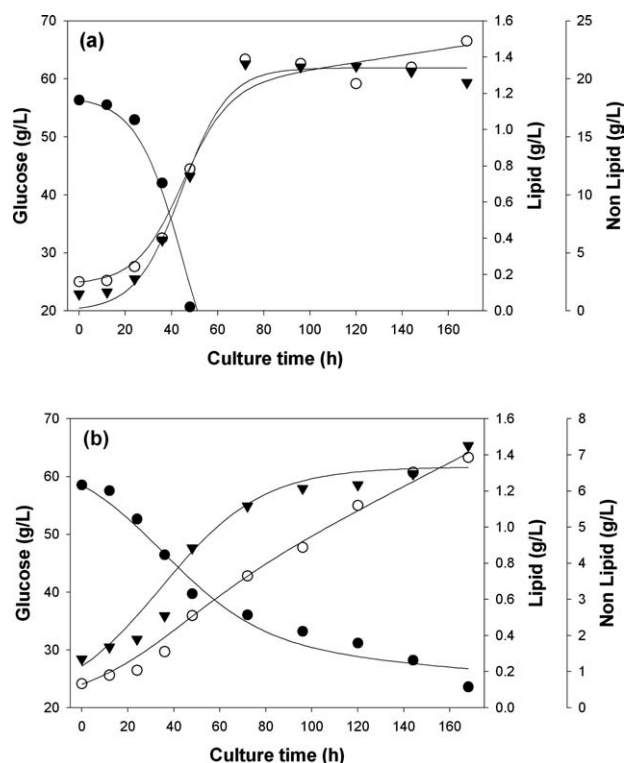


**Figure 4.** Comparison of model predictions (solid line) and experimental data for nonlipid biomass (closed triangle), lipid (open circle), and glucose consumption (closed circle) at (a) C:N ratio 10:1 and 60 g L<sup>-1</sup> glucose loading and (b) C:N ratio 70:1 and 60 g L<sup>-1</sup> glucose loading.

multiplication and total biomass increase than the actual increase in cellular lipid content. This statement could also be supported by the relative magnitudes of the empirical parameters  $m$  and  $n$ , where in all C:N ratios,  $m$  values were greater than  $n$ , suggesting that lipid production by activated sludge microbiota was mixed growth-associated with greater

contributions from the growth-associated lipid production term.<sup>33</sup> This could be the case in the C:N both 40:1 and 70:1 treatment runs, wherein the overall and stationary phase (3–7 d)  $Y_{P/S}$  values were not significantly different. These parameters, however, were both significantly higher than those obtained from C:N ratio 10:1.

In summary, it could be concluded that a low C:N (10:1) favored nonlipid biomass production, whereas a high C:N (70:1) favored lipid accumulation. However, to attain maximal volumetric lipid yields, nonlipid biomass yields need to be enhanced as well to provide sufficient cellular vehicles that contain the accumulated lipids. Based on the results, C:N 40:1 and 60 g L<sup>-1</sup> glucose loading produced higher volumetric lipid yields in a batch cultivation due to its sufficiently higher  $Y_{X/S}$  and a  $Y_{P/S}$  that is comparable to C:N 70:1.

### Effect of glucose loading

Previous studies on oleaginous yeasts indicated that maximum  $Y_{P/S}$  values were obtained at high C:N and low sugar concentrations, whereas  $Y_{X/S}$  is affected only by the C:N ratio.<sup>34,35</sup> Biomass concentration profiles (Figure 3a) as well as  $Y_{X/S}$  and  $\mu_{max}$  values (Table 2) were not significantly different between the 40 and 60 g L<sup>-1</sup> treatments. The total biomass concentration increased continuously and the lag, exponential, and stationary phases were not distinguishable from each other in the growth curves. When using 20 g L<sup>-1</sup>, however, the lag and exponential phases occurred within 3 d followed by a very distinct stationary phase. The  $Y_{X/S}$ ,  $X_{max}$ , and  $\mu_{max}$  values for this initial glucose concentration were also lower than those from 40 and 60 g L<sup>-1</sup>, which might have been caused by relatively low initial nitrogen levels supplied.

Glucose consumption profiles (Figure 3b) were also similar among the three initial glucose concentrations investigated, with an increasing amount of fermentation time needed for complete utilization. NH<sub>4</sub><sup>+</sup>-N concentration profiles (Figure 3c) were also similar, with nitrogen limitation occurring after 1 d at 20 g L<sup>-1</sup> initial glucose, and 2 d at 40 and 60 g L<sup>-1</sup> initial glucose. Gravimetric lipid content profiles (Figure 3d) were also statistically similar for all three

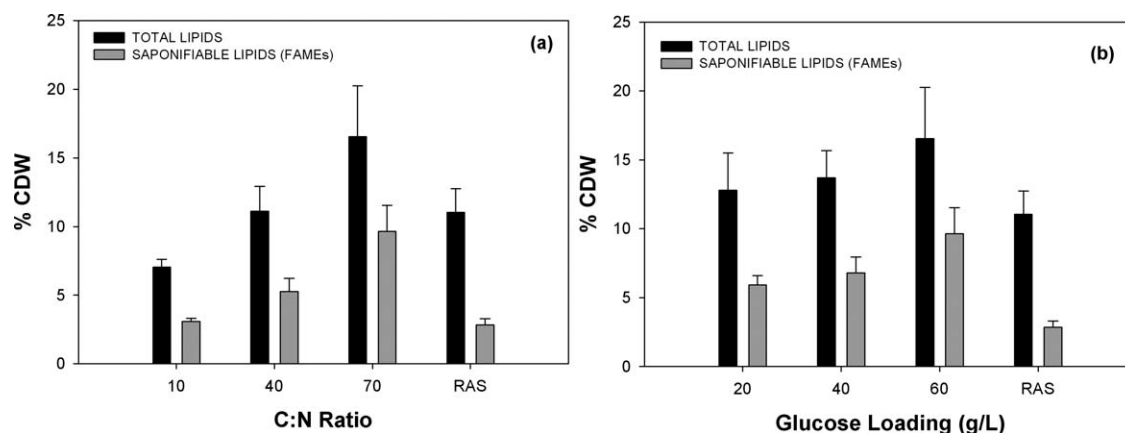


**Figure 5.** Total lipids and saponifiable fractions in activated sludge-derived lipids ( $t = 7$  d) for biodiesel production. RAS: raw activated sludge.

**Table 2. Kinetic Parameter Estimates and 90% Confidence Levels for the Proposed Model**

Parameter	Initial C:N Ratio				
	10:1	40:1	70:1	70:1	70:1
	Initial Glucose Loading (g L <sup>-1</sup> )				
	60	60	60	40	20
Nonlipid biomass					
$\mu_{\max}$ (h <sup>-1</sup> )	0.100 ± 0.002	0.052 ± 0.022	0.046 ± 0.019	0.043 ± 0.01	0.034 ± 0.0003
$X_0$ (g L <sup>-1</sup> )	0.241 ± 0.024	1.41 ± 1.15	1.15 ± 0.62	1.66 ± 0.41	1.33 ± 0.01
$X_{\max}$ (g L <sup>-1</sup> )	20.9 ± 0.3	16.5 ± 1.66	6.66 ± 0.64	7.48 ± 0.39	3.65 ± 0.01
$R^2$	0.990	0.974	0.959	0.989	0.920
Lipid accumulation					
$m$ (g lipid g <sup>-1</sup> nonlipid)	0.051 ± 0.008	0.066 ± 0.012	0.080 ± 0.027	0.11 ± 0.02	0.099 ± 0.036
$10^5 n$ (g lipid g <sup>-1</sup> nonlipid h <sup>-1</sup> )	9.35 ± 9.31	48.8 ± 13.4	9.77 ± 2.45	45.4 ± 17.0	35.4 ± 23.2
$P_{\max}$ (g L <sup>-1</sup> *)	1.49 ± 0.08 (7)	2.24 ± 0.51 (7)	1.39 ± 0.08 (7)	1.23 ± 0.08 (7)	0.52 ± 0.13 (7)
$R^2$	0.994	0.997	0.997	0.998	0.987
Glucose consumption					
$\alpha$ (g glucose g <sup>-1</sup> nonlipid)	2.54 ± 0.58	3.49 ± 0.33	5.03 ± 1.21	4.08 ± 1.54	6.29 ± 3.93
$10^3 \beta$ (g glucose g <sup>-1</sup> nonlipid h <sup>-1</sup> )	8.19 ± 19.6	2.49 ± 3.69	0.483 ± 1.11	18.7 ± 13.1	39.2 ± 35.7
Overall $Y_{X/S}$ (g nonlipid g <sup>-1</sup> glucose)	0.354 ± 0.019	0.274 ± 0.017	0.167 ± 0.007	0.166 ± 0.004	0.113 ± 0.025
Overall $Y_{P/S}$ (g lipid g <sup>-1</sup> glucose)	0.024 ± 0.003	0.034 ± 0.007	0.038 ± 0.010	0.027 ± 0.003	0.020 ± 0.006
Stationary phase $Y_{P/S}$ (g lipid g <sup>-1</sup> glucose)	0.024 ± 0.003	0.054 ± 0.024	0.063 ± 0.030	0.026 ± 0.004	0.019 ± 0.006
$R^2$	0.990	0.987	0.975	0.978	0.912

\*Values in parentheses indicate fermentation time elapsed in (h) which  $P_{\max}$  was attained.

treatments, exhibiting an initial degradation up to 2 d followed by an increasing trend, which coincided with the depletion of residual  $\text{NH}_4^+\text{--N}$  in the culture. This was to be expected, because all the initial glucose levels investigated have the same initial C:N ratios. However, in terms of volumetric lipid concentrations (Figure 3f), only initial glucose levels of 40 and 60 g L<sup>-1</sup> produced similar increasing trends as a result of their statistically similar biomass growth and lipid accumulation profiles. At 20 g L<sup>-1</sup>, lipid concentrations reached a plateau after 3 d (Figure 3f) due to the observed cessation of biomass production (Figure 3a). As shown in Table 2, the overall and stationary (lipid accumulation) phase  $Y_{P/S}$  values were not significantly different as the 90% confidence limits of these parameter estimates overlapped.  $P_{\max}$  values were statistically similar at 40 and 60 g L<sup>-1</sup> initial glucose levels and lowest at 20 g L<sup>-1</sup>. Although all three initial glucose levels were operated under the same C:N ratio of 70:1, which according to the results of the earlier experiments was conducive to lipid accumulation in activated sludge microorganisms, the low initial glucose supply of 20 g L<sup>-1</sup> was depleted quickly along with the  $\text{NH}_4^+\text{--N}$ , leaving no residual carbon for lipid synthesis. Lipid production was also found to be growth associated ( $m > n$ ) for all initial glucose levels and glucose consumption profiles were also very similar with the time elapsed for glucose depletion increasing with increasing glucose loading (Figure 3b). From these observations, it is evident that at C:N 70:1, glucose loadings of 40 or 60 g L<sup>-1</sup> are favorable for enhancing both biomass yield and gravimetric lipid content, which has a combined influence in the resulting volumetric lipid yield. Similarly designed experiments involving a pure culture of the oleaginous yeast *R. gracilis* in previous studies<sup>21,22</sup> showed similar  $\mu_{\max}$ ,  $Y_{X/S}$ , and  $X_{\max}$  estimates with those obtained using activated sludge microorganisms in this study. However, at similar experimental conditions (C:N 70, 60 g L<sup>-1</sup> glucose), the maximum  $P_{\max}$  and  $Y_{P/S}$  of cultured

activated sludge (1.41 g L<sup>-1</sup>, 0.038 g g<sup>-1</sup> glucose overall, 0.0667 g g<sup>-1</sup> glucose at stationary phase) were lower than the values obtained from *R. gracilis* (11.60 g L<sup>-1</sup>, 0.19 g g<sup>-1</sup> glucose).

### Model validation

To test the reliability of the proposed models for nonlipid biomass production, lipid accumulation, and glucose utilization of activated sludge, the nonlinear regression-estimated parameters (Table 2) were used to simulate the model with the 4th/5th order Runge–Kutta method. Experimental and simulated values were compared in representative plots (Figure 4). Coefficients of determination ( $R^2$ ) values were also calculated for each treatment (Table 2) and in all cases,  $R^2$  values were greater than 0.90. Some limitations of the proposed model that may account for the 10% difference could be the assumption by the logistic model that no endogenous metabolism or degradation of cellular material occurs, hence only saturation levels are reported from the stationary phase up to  $t = \infty$ .<sup>23</sup> The Luedeking–Piret model predictions for lipid production also failed to predict slight decreases in the lipid concentration particularly at C:N 10:1 (Figure 2a), as a result of endogenous utilization of the stored lipids for cell maintenance due to depletion of the primary carbon source (glucose).<sup>21</sup> As a result, it would be useful to incorporate cell death phase kinetics and degradation of storage lipids as an endogenous carbon source in future models.

### FAME analysis

Results from GC-FID analysis indicate that the saponifiable lipid fraction/biodiesel yield increased proportionally and exhibited the same trend with the total gravimetric lipid yield with respect to C:N ratio and glucose loading (Figure 5). In all cases, the saponifiable fractions of glucose-grown activated sludge biomass constituted 50–60% of the total



**Table 3. Relative Fatty Acid Composition (% w/w total FAMES) of Activated Sludge-Derived Oil**

Fatty Acid Residue	Raw Activated Sludge	Initial C:N Ratio				
		10:1	40:1	70:1	70:1	70:1
		Initial glucose loading (g L <sup>-1</sup> )				
		60	60	60	40	20
Palmitate, C16:0	16.0	14.6	20.5	21.2	21.7	21.7
Palmitoleate, C16:1	14.9	5.29	4.17	2.48	2.53	3.72
Stearate, C18:0	7.68	5.35	11.1	13.8	15.0	15.6
Oleate, C18:1	22.8	42.9	42.2	36.9	39.1	38.4
Linoleate, C18:2	7.68	18.6	11.9	17.1	13.4	11.6
Linolenate, C18:3	1.62	6.71	2.02	1.96	1.88	1.73
Unknowns	25.4	4.74	6.16	4.4	4.79	5.31

extracts, compared to only 25% in RAS, suggesting an increase in viability of the sludge lipid extracts for biofuel feedstock application. The highest biodiesel yield ( $10.2 \pm 2.0\%$  CDW) was obtained at C:N 70, 60 g L<sup>-1</sup> glucose loading after 6 d of fermentation and corresponds to a total lipid extract yield of around 18% CDW compared to  $2.84 \pm 0.45\%$  CDW biodiesel and  $11.0 \pm 1.7\%$  CDW total lipids from RAS.

The major fatty acyl residues affected by glucose-fed aerobic fermentation were palmitic (C16:0), palmitoleic (C16:1), stearic (C18:0), oleic (C18:1), linoleic (C18:2), and linolenic (C18:3) acids (Table 3). For RAS oil, majority of the fatty acids consists (in % w/w of total saponifiable lipids) of unsaturated fatty acids oleate (22) and palmitoleate (14.9) followed closely by the saturated fatty acid palmitate (16), and about 25% of unclassified residues. Following aerobic glucose fermentation, the proportion of unsaturated fatty acids increased to ~70% in all the treatments investigated, and the percentage of unclassified FAMES was reduced to an average of 5%. The majority of the unsaturated fatty acids in glucose-grown activated sludge were composed of oleic acid, whose levels were on average nearly twice those from RAS (i.e., 40 vs. 22.8%). Different trends have also been observed for each type of fatty acyl residue as an effect of varying initial C:N ratio and glucose loading. Palmitic and stearic acid levels generally increased with increasing initial C:N ratio, with slightly higher levels at lower initial glucose loadings. On the other hand, levels of the unsaturated fatty acids palmitoleate, oleate, linoleate, and linolenate generally decreased slightly with increasing C:N ratio and remained fairly constant with changing initial glucose loading. Regardless of C:N ratio or glucose loading, oleic acid was found to be the dominant fatty acyl residue (38–43%) in glucose-grown activated sludge. This is a significant improvement from raw sludge (23% oleic acid) in terms of balancing cold flow and oxidative stability and enhancing the ignition quality (cetane number) of sludge biodiesel which can be attributed to oleic acid levels.<sup>36</sup>

### Microbial community analysis

Although the composition of activated sludge microbiota has been studied previously,<sup>37</sup> to our knowledge this is the first time sludge microbial communities have been studied under conditions conducive to enhanced lipid accumulation. 16S rRNA gene clone libraries were developed from the

samples obtained at different C:N ratios (Table 4), because it had a significant effect on lipid accumulation in activated sludge. Similar to previous studies<sup>38,39</sup> members of the Proteobacteria (Gram-negative bacteria) phylum dominated the raw sludge samples prior to the treatments (58.4%). Specifically, gamma-(23.7%) and beta-like (17.2%) sequences were the dominant Proteobacteria. Alpha- and delta-like Proteobacteria sequences were ~8% each. Bacteroidetes were also numerically dominant representing 26.6% of the total sequences analyzed, most of which were closely related to Sphingobacteria. Verrucomicrobia-like sequences were close to 7%, whereas other groups represented less than 1% each (i.e., Gram-positive bacteria or Firmicutes, TM7, Gemmatimonadetes, OP10, SR1, Chloroflexi).

Significant changes in microbial composition were observed for each of the treatments after 3 d, which corresponded to the onset of the stationary phase and lipid accumulation in the case of C:N 70:1. At C:N 10:1 and C:N 40:1, Firmicutes increased from 0.6 to 67 and 65% of all sequences, respectively. Most Firmicutes sequences (78–86%) were closely related to members of the Clostridia class. Proteobacteria decreased considerably in numbers, representing less than 18% (i.e., 7.8% for C:N 10:1 and 17.8% for C:N 40:1) of the sequences, most of which were gamma-like sequences. In contrast, Actinobacteria increased to 7.8 and 5.9% in C:N 10:1 and C:N 70:1 clone libraries, respectively. No Bacteroidetes sequences were found in any of the treatments after 3 d. The C:N 70:1 community was vastly dominated by Proteobacteria (96%) after 3 d, most of which were gammaproteobacteria (150 out of 168 sequences). Some of the most abundant gammaproteobacteria were members of Enterobacteriales, Pseudomonadales, and Aeromonadales, which were below detection limits in the initial sludge community. In a previous study, some members of these orders (genera *Pseudomonas* and *Aeromonas*) have been isolated from municipal sewage sludge as producers of polyhydroxyalkanoates under similar conditions with this article.<sup>40</sup> Further, extracellular polysaccharide formation has been detected in bacteria of the orders Rhodospirillales, Sphingomonadales, Xanthomonadales, Enterobacteriales, and Pseudomonadales.<sup>41</sup> These microbial storage products could take into account the unsaponifiable fraction of the lipids not converted to biodiesel.

After 7 d, *Clostridia*-like sequences were again numerically dominant in C:N 10:1 and C:N 40:1 (i.e., 80%) clone libraries, with *Sporacetigenium*- and *Turicibacter*-like sequences

**Table 4. Relative Abundance of Bacteria Groups in Raw and Cultured Activated Sludge at Different Initial C:N Ratios**

Phylum	Class	Order	% of Total Sequences					
			Day 0	Day 3	Day 7	Day 3	Day 7	Day 3
			RAS	C:N 10:1	C:N 10:1	C:N 40:1	C:N 40:1	C:N 70:1
Proteobacteria	Gammaproteobacteria	Aeromonadales	–	1.2	–	2.7	1.1	26.3
		Enterobacteriales	–	4.8	–	3.8	–	32.6
		Pseudomonadales	0.4	0.6	–	2.2	0.5	20.6
		Legionellales	0.4	–	–	–	–	–
		Xanthomonadales	22.6	0.6	–	0.5	0.5	–
		Unclassified	0.4	–	–	1.1	0.5	6.9
	Alphaproteobacteria	Rhodospirillales	0.4	–	–	1.6	–	4.0
		Rhizobiales	1.5	–	–	–	–	0.6
		Rhodobacterales	2.6	–	–	–	–	–
		Caulobacteriales	0.4	–	–	–	–	–
		Sphingomonadales	1.8	–	–	–	0.5	–
		Rickettsiales	0.4	–	–	–	–	–
		Unclassified	1.5	–	–	–	–	–
	Betaproteobacteria		17.2	0.6	0.6	1.6	1.6	2.9
	Deltaproteobacteria		7.7	–	–	–	–	–
	Epsilonproteobacteria		–	–	–	–	–	0.6
Verrucomicrobia	Unclassified		1.5	–	–	4.3	–	1.1
	Opitutae		0.4	–	–	–	–	–
	Verrucomicrobiae		6.2	–	–	–	–	–
	Subdivision 3		0.4	–	–	–	–	–
Bacteroidetes	Flavobacteria		2.9	–	–	–	0.5	–
	Sphingobacteria		22.6	–	–	–	–	–
	Unclassified		1.1	–	–	–	–	–
Firmicutes	Bacilli		–	0.6	–	0.5	–	2.3
	Erysipelotrichi		–	9.0	16.1	13.0	13.1	0.6
	Clostridia		0.4	57.2	81.1	50.8	66.1	0.6
	Unclassified		–	–	–	0.5	–	–
Actinobacteria			0.4	7.8	1.7	5.9	12.0	–
Unclassified bacteria			3.6	17.5	0.6	8.1	1.6	0.6
Total sequences			274	166	180	185	183	175

being the most dominant. Similar to other *Clostridia*, *Sporacetigenium*, and *Turicibacter* type species are considered obligate anaerobic bacteria. The fact that these microorganisms dominated in aerated bioreactors suggest that some of their close relatives might be aerotolerant or that there are micro-niches within these systems that can promote anaerobic growth. The changes in composition favoring *Clostridia* as abundant bacteria in the C:N 10:1 and C:N 40:1 samples can be explained by the utilization of potentially available carbohydrates such as glycerol, a process that could result in the production of value added products such as butanol.<sup>42</sup>

Nearly all of the C:N 70:1 sequences (99%) were alphaproteobacteria after 7 d, indicating a significant shift in microbial composition, specifically from gamma- to alphaproteobacteria. Most of the alpha-like sequences were closely related to *Acidomonas methanolytica*, a member of the Rhodospirillales order. Interestingly, no *Acidomonas*-related sequences were detected in the initial sludge community. While the microbial composition was different at 7 d between low/medium C:N and high C:N ratios, the results also suggest that prolonged exposure to any of these conditions could lead to the significant reduction in the diversity of the activated sludge microbiota, a fact that might influence the net lipid production yields. Besides the accumulation of fermentation by-products, the decreased pH of the culture (from 6.5 at 0 d to 2.0 at 3 d onward) could have also influenced bacterial survival at high C:N ratios, as *Acidomonas* is known to grow under low pH conditions.

The bacterial groups responsible for lipid production, specifically the saponifiable fraction, in these consortia have yet to be conclusively determined, although some of the potential bacterial groups were identified. Indeed, the molecular data will allow these groups to be further studied using quantitative group-specific assays. On one hand, it is possible that not all members of the community are contributing in a similar manner to lipid production. On the other hand, complex microbial interactions are presumed to play important roles in diverse microbial communities such as activated sludge. In this regard, understanding the microbial composition of amended activated sludge samples is relevant to develop functionally stable engineered systems.

## Conclusions

It can be concluded from this article that cultivation of activated sludge microorganisms in high initial C:N ratio (>40:1) and glucose loading ( $\geq 40$  g L<sup>-1</sup>) aerobic bioreactors has been shown to enhance gravimetric lipid and biodiesel yields in municipal sewage sludge. Volumetric lipid yields, however, were highest at C:N 40:1 than C:N 70:1 due to a higher total biomass yield in the former. The maximum gravimetric lipid yield of  $17.5 \pm 3.9\%$  CDW with a corresponding biodiesel yield to  $10.2 \pm 2.0\%$  CDW was obtained at C:N 70:1 and glucose loading of 60 g L<sup>-1</sup>. These values are significantly higher than those

obtained in RAS ( $11.0 \pm 1.7\%$  CDW total lipids,  $2.84 \pm 0.45\%$  CDW biodiesel yield). The resulting fatty acid profiles indicated that lipids derived from activated sludge grown aerobically in glucose-containing synthetic wastewater medium is suitable for the production of biodiesel with improved cold flow, ignition property (cetane number), and oxidative stability.

Mathematical modeling of nonlipid production, lipid accumulation, and glucose consumption using the Logistic and Luedeking–Piret equations indicated a good correlation between the experimental data and model simulations. Analysis of the kinetic parameter estimates concluded that lipid production in activated sludge microbiota was mixed growth associated with total biomass production exerting a greater influence than actual increases in the lipid contents of individual cells. Hence, for process optimization of batch aerobic fermentation of glucose using activated sludge, nonlipid biomass yields need to be considered in addition to gravimetric lipid yields. Further studies must be conducted to enhance nongrowth-associated lipid production as well to improve cellular lipid contents and yield.

Analysis of the composition of activated sludge microbial community via 16S rRNA sequencing concluded that glucose-fed aerobic fermentation resulted in the reduction of microbial diversity in activated sludge microbiota toward more specific classes of microorganisms. The information derived from this analysis could assist in identifying and isolating potential lipid-producing microorganisms in activated sludge and modify the composition of the sludge microbiota accordingly to further maximize lipid biodiesel yields.

Recent estimates indicate that this proposed process could potentially increase the annual biodiesel yield from sewage sludge to 10 billion gallons, which is more than three times the United States' current biodiesel production capacity.<sup>8</sup> Additionally, using naturally occurring microbial consortia such as activated sludge for the production of biofuel feedstock lipids could prove to be beneficial in that it may eliminate the need for media sterilization as opposed to working with pure cultures. Furthermore, the results have shown that some members of wastewater microbial communities are capable of accumulating lipids under extreme conditions such as low culture pH unlike pure cultures of oleaginous microorganisms, providing support on the use of mixed microbial cultures over single strains for the production of biofuel feedstock. The production of high-value chemicals could also potentially offset wastewater treatment costs or serve as additional income for municipalities operating these wastewater treatment facilities.

## Acknowledgments

The authors would like to thank the U.S. Department of Energy and U.S. Environmental Protection Agency Regional Applied Research (RARE) program for providing the funding for this research. This paper was developed under Cooperative Agreement No. CR-83361801 awarded by the U.S. Environmental Protection Agency. EPA made comments and suggestions on the document intended to improve the scientific analysis and technical accuracy of the document. However, the views expressed in this document are those of Mississippi State University and EPA does not endorse any products or commercial services mentioned in this publication.

## Literature Cited

1. Biomass Research and Development Board. National Biofuels Action Plan. Available at: <http://www1.eere.energy.gov/biomass/> [Accessed December 2, 2008].
2. Knothe G. *Introduction: what is biodiesel?* In: Knothe G, Van Gerpen J, Krahl J, editors. *The Biodiesel Handbook*. Champaign, IL: AOCS Press, 2005:1–3.
3. Donnis B, Egeberg RG, Blom P, Knudsen KG. Hydroprocessing of bio-oils and oxygenates to hydrocarbons. Understanding the reaction routes. *Top Catal*. 2009;52:229–240.
4. Stumborg M, Wong A, Hogan E. Hydroprocessed vegetable oils for diesel fuel improvement. *Bioresour Technol*. 1996;56:13–18.
5. National Renewable Energy Laboratory. Biomass Oil Analysis: Research Needs and Recommendation. Available at: <http://www1.eere.energy.gov/biomass/pdfs/34796.pdf> [Accessed December 2, 2008].
6. Food and Agricultural Organization, United Nations. FAO's Views on Bioenergy. Available at: <http://www.fao.org/bioenergy/47280/en/> [Accessed January 9, 2011].
7. Haas MJ, Foglia TA. *Alternate feedstocks and technologies for biodiesel production*. In: Knothe G, Krahl J, Van Gerpen J, editors. *The Biodiesel Handbook*. Champaign, IL: AOCS Press, 2005:42–61.
8. Kargbo DM. Biodiesel production from municipal sewage sludges. *Energ Fuel*. 2010;24:2791–2794.
9. Dufreche S, Hernandez R, French T, Sparks D, Zappi M, Alley E. Extraction of lipids from municipal wastewater plant microorganisms for production of biodiesel. *J Am Oil Chem Soc*. 2007;84:181–187.
10. Mondala A, Liang K, Toghiani H, Hernandez R, French T. Biodiesel production by *in situ* transesterification of municipal primary and secondary sludges. *Bioresour Technol*. 2009;100:1203–1210.
11. Revellame E, Hernandez R, French W, Holmes W, Alley E. Biodiesel from activated sludge through *in situ* transesterification. *J Chem Technol Biotechnol*. 2010;85:614–620.
12. U.S. Environmental Protection Agency. Biosolid Generation, Use, and Disposal in the United States. Available at: <http://www.biosolids.org/docs/18941.PDF> [Accessed January 12, 2009].
13. Ratledge C. *Single cell oils for the 21st century*. In: Cohen Z, Ratledge C, editors. *Single Cell Oils*. Champaign, IL: AOCS Press, 2005:1–20.
14. Ratledge C, Wynn JP. The biochemistry and molecular biology of lipid accumulation in oleaginous microorganisms. *Adv Appl Microbiol*. 2002;51:1–51.
15. Ghosh S, LaPara TM. Removal of carbonaceous and nitrogenous pollutants from a synthetic wastewater using a membrane-coupled bioreactor. *J Ind Microbiol Biotechnol*. 2004;31:353–361.
16. DIONEX. Dionex Corp. Application Note 141: Determination of inorganic cations and ammonium in environmental waters by ion chromatography using the CS16 IonPac column. Available at: [http://www.dionex.com/en-us/webdocs/4211\\_AN141\\_V15.pdf](http://www.dionex.com/en-us/webdocs/4211_AN141_V15.pdf) [Accessed August 1, 2008].
17. Bligh EG, Dyer WJ. A rapid method for total lipid extraction and purification. *Can J Biochem Physiol*. 1959;37:911–917.
18. Christie WW. *Lipid analysis: Isolation, Separation, Identification, and Structural Analysis of Lipids*, 3rd ed. Bridgewater, England: The Oily Press, 2003.
19. Klimek J, Ollis DF. Extracellular microbial polysaccharides: kinetics of *Pseudomonas* sp., *Azotobacter vinelandii*, and *Aureobasidium pullulans* batch fermentations. *Biotechnol Bioeng*. 1980;22:2321–2342.
20. Weiss RM, Ollis DF. Extracellular microbial polysaccharides. I. Substrate, biomass, and product kinetic equations for batch xanthan gum fermentation. *Biotechnol Bioeng*. 1980;22:859–873.
21. Karanth NG, Sattur AP. Mathematical modeling of production of microbial lipids. Part II: Kinetics of lipid accumulation. *Bioprocess Eng*. 1991;6:241–248.
22. Sattur AP, Karanth NG. Mathematical modeling of production of microbial lipids. Part I: Kinetics of biomass growth. *Bioprocess Eng*. 1991;6:227–234.
23. Shuler ML, Kargi F. *Bioprocess Engineering Basic Concepts*, 2nd ed. Saddle River, NJ: Prentice-Hall, Inc., 2002.
24. Yan S, Subramanian B, Surampalli RY, Narasiah S, Tyagi RD. Isolation, characterization, and identification of bacteria from activated sludge and soluble microbial products in wastewater treatment systems. *Pract Periodical Haz Toxic Radioactive Waste Mgmt*. 2007;11:240–258.

25. Lamendella R, Santo Domingo JW, Yannarell AC, Ghosh S, Di Giovanni G, Mackie RI, Oerther DB. Evaluation of swine-specific PCR assays used for fecal source tracking and analysis of molecular diversity of swine-specific "*Bacteroidales*" populations. *Appl Environ Microbiol.* 2009;75:5787–5796.
26. Cole JR, Wang Q, Cardenas E, Fish E, Chai B, Farris RJ, Kulam-Syed-Mohideen AS, McGarrell DM, Marsh T, Garrity GM, Tiedje JM. The Ribosomal Database Project: improved alignments and new tools for rRNA analysis. *Nucleic Acids Res.* 2008;37:D141–D145.
27. Sattur AP, Karanth NG. Production of microbial lipids: I. Development of a mathematical model. *Biotechnol Bioeng.* 1989;34:863–867.
28. Davies RJ, Holdsworth JE. *Synthesis of lipids in yeasts biochemistry, physiology, production.* In: Padley FB, editor. *Advances in Applied Lipid Research 1.* Greenwich, CT: JAI Press Ltd., 1992:119–159.
29. Allen LA, Barnard NH, Fleming M, Hollis B. Factors affecting the growth and fat formation of *Rhodotorula gracilis*. *J Appl Bact.* 1963;27:27–40.
30. Liden G, Jacobsson V, Niklasson C. The effect of carbon dioxide on xylose fermentation by *Pichia stipitis*. *Appl Biochem Biotechnol.* 1993;38:27–40.
31. Davies RJ. *Yeast oil from cheese whey-process development.* In: Morerton RS, editor. *Single Cell Oil.* London: Longmans, 1988:99–145.
32. Wayman M, Jenkins AD, Kormendy AG. *Bacterial production of fats and oils.* In: Ratledge C, Dawson P, Rattray J, editors. *Biotechnology for the Oils & Fats Industry.* Champaign, IL: AOCS Press, 1984:129–144.
33. Don MM, Shoparwe NF. Kinetics of hyaluronic acid production by *Streptococcus zooepidemicus* considering the effect of glucose. *Biochem Eng J.* 2010;49:95–103.
34. Sattur AP, Karanth NG. Production of microbial lipids: II. Influence of C/N ratio—model prediction. *Biotechnol Bioeng.* 1989;34:868–871.
35. Sattur AP, Karanth NG. Production of microbial lipids. III: Influence of C/N ratio—experimental observations. *Biotechnol Bioeng.* 1989;34:872–874.
36. Bringe NA. *Soybean oil composition for biodiesel.* In: Knothe G, Krahl J, Van Gerpen J, editors. *The Biodiesel Handbook.* Champaign, IL: AOCS Press, 2005:161–164.
37. Snaird J, Amann R, Huber I, Ludwig W, Schleifer KH. Phylogenetic analysis and *in situ* identification of bacteria in activated sludge. *Appl Environ Microbiol.* 1997;63:2884–2896.
38. Wagner M, Amann R, Lemmer H, Schleifer KH. Probing activated sludge with oligonucleotides specific for Proteobacteria: inadequacy of culture-dependent methods describing microbial community structure. *Appl Environ Microbiol.* 1993;59:1520–1525.
39. Eschenhagen M, Schuppler M, Roske I. Molecular characterization of the microbial community structure in two activated sludge systems for the advanced treatment of domestic effluents. *Water Res.* 2003;37:3224–3232.
40. Reddy SV, Thirumala M, Reddy TVK, Mahmood SK. Isolation of bacteria producing polyhydroxyalkanoates (PHA) from municipal sewage sludge. *World J Microbiol Biotechnol.* 2008;24:2949–2955.
41. Vu B, Chen M, Crawford RJ, Ivanova EP. Bacterial extracellular polysaccharides involved in biofilm formation. *Molecules.* 2009;14:2535–2554.
42. Taconi KA, Venkataramanan KP, Johnson DT. Growth and solvent production by *Clostridium pasteurianum* ATCC 6013 utilizing biodiesel-derived crude glycerol as the sole carbon source. *Environ Prog Sust Energ.* 2009;28:100–110.

Manuscript received Aug. 10, 2010, and revision received Mar. 18, 2011.